ACCSCIENCE PUBLISHING

Tumor Discovery

ORIGINAL RESEARCH ARTICLE

Homoharringtonine inhibits pancreatic cancer progression via mitochondrial energy metabolism suppression and macrophages reduction

Xiaoxia Wang, Tao Wang, Xuelu Peng, Ke Zhu, Ming Ye, Jie Meng*, and Haiyan Xu*

Department of Biomedical Engineering, Institute of Basic Medical Sciences, Chinese Academy of Medical Sciences and Peking Union Medical College, Beijing, China

Abstract

Homoharringtonine (HHT) has been used in leukemia therapy since the 1970s. Its inhibitory effects on solid tumors have attracted increasing interest and have been actively explored in recent years. This study investigates the therapeutic effects and pharmacological mechanisms of HHT on pancreatic cancer, focusing on mitochondrial energy metabolism and macrophage sensitivity to HHT. HHT significantly inhibited the proliferation and colony formation of pancreatic cancer cell lines PANC-1 and Pan02 *in vitro* and suppressed tumorigenic potential *in vivo*. The mechanistic study revealed that HHT induced a significant elevation of reactive oxygen species (ROS) levels in pancreatic cancer cells over time, as evidenced by the enhanced dichlorodihydrofluorescein diacetate fluorescence and an elevated NAD^+/NADH ratio. This resulted in mitochondrial respiratory dysfunction, including reductions in basal respiration, maximal respiration, and adenosine triphosphate production. In addition, HHT caused cell cycle arrest and disrupted the cytoskeleton, thereby inhibiting cell division and proliferation. The anti-tumor effects of HHT were further evaluated using a subcutaneous pancreatic tumor-bearing mouse model, showing that HHT inhibited the proliferation of pancreatic tumor cells *in vivo*, which led to reduced tumor mass. Moreover, HHT significantly reduced the viability of macrophages both *in vitro* and *in vivo*, leading to the depletion of tumor-associated macrophages in the tumor microenvironment (TME), thereby alleviating immune suppression. In conclusion, HHT effectively inhibits pancreatic cancer progression through upregulating cellular ROS levels over time, thereby disrupting mitochondrial respiratory capacity in tumor cells and reducing macrophage populations, contributing to TME reprogramming and immune restoration.

Keywords: Pancreatic cancer; Reactive oxygen species; Mitochondrial energy metabolism; Cell cycle; Tumor microenvironment

***Corresponding authors:**
Haiyan Xu
(xuhy@pumc.edu.cn)
Jie Meng
(mengjie@ibms.pumc.edu.cn)

Citation: Wang X, Wang T, Peng X, *et al*. Homoharringtonine inhibits pancreatic cancer progression via mitochondrial energy metabolism suppression and macrophages reduction. *Tumor Discov*. 2025;4(1):99-112.
doi: 10.36922/td.7825

Received: December 17, 2024

Revised: January 20, 2025

Accepted: January 24, 2025

Published online: February 24, 2025

Copyright: © 2025 Author(s). This is an Open-Access article distributed under the terms of the Creative Commons Attribution License, permitting distribution, and reproduction in any medium, provided the original work is properly cited.

Publisher's Note: AccScience Publishing remains neutral with regard to jurisdictional claims in published maps and institutional affiliations.

1. Introduction

Pancreatic cancer is a malignant tumor of the digestive system with high lethality and low cure rates. It is the sixth leading cause of cancer-related deaths in China[1] and

ranks 12th in new cases but sixth in cancer mortality worldwide.[2] Among pancreatic cancers, pancreatic ductal adenocarcinoma (PDAC) has one of the highest mortality rates among solid tumors, with an overall 5-year survival rate of <10%.[3] Pancreatic tumors treated with standard chemotherapy regimens are prone to developing drug resistance, whose mechanisms are further complicated by the genetic heterogeneity of the tumors.[4] Moreover, drug resistance in pancreatic cancer is not only driven by intrinsic tumor cell mechanisms but also by immune suppression within the tumor microenvironment (TME).[5-8] Therefore, more effective therapeutic approaches are keen to address the challenges in improving pancreatic cancer treatment outcomes.

Homoharringtonine (HHT), an alkaloid extracted from the herb *Cephalotaxus*, is a protein synthesis inhibitor that inhibits the initial elongation step of translation by binding to the A-site of the ribosome, thereby inhibiting protein synthesis.[9,10] HHT has been approved by the U.S. Food and Drug Administration for the treatment of chronic myeloid leukemia (CML) and acute myeloid leukemia (AML).[11,12] In recent years, studies on HHT have expanded to solid tumors. Several pioneering investigations have shown that HHT exerts inhibitory effects on the growth of human pancreatic cancer cells, such as inhibiting proliferation and growth of MIA-PaCa-2 and PANC-1 cells in a time- and dose-dependent manner.[13,14] In addition, HHT has been shown to induce cell cycle arrest and enhance the anticancer activity of erlotinib in MIA-PaCa-2 and B×PC-3 cells.[15] Nevertheless, despite its promising potential in pancreatic cancer therapy, the underlying molecular mechanisms and therapeutic efficacy of HHT require further investigation.

Previous studies on CML cells have indicated that HHT affects mitochondrial functions, particularly in oxygen consumption rate (OCR).[16] This implies the involvement of reactive oxygen species (ROS), which plays a crucial role in maintaining cellular homeostasis in normal cells. However, ROS dysregulation in cancer cells often leads to aberrant cell signaling and uncontrolled proliferation.[17-19] Building on this evidence, this study investigated the potential anti-tumor effects of HHT on PDAC cells and its underlying mechanism of action, focusing on mitochondrial energy metabolism in both tumor cells and stromal cells within the TME. The results showed that HHT significantly inhibited pancreatic cancer progression through significantly elevating intracellular ROS levels over time, resulting in the disruption of mitochondrial respiratory capacity, impairment of energy metabolism, and cell cycle arrest. In addition, HHT alleviated the immunosuppressive effects within the TME by reducing the viability of macrophages.

2. Materials and methods

2.1. Cells, reagents, and animal models

Human pancreatic cancer cell lines PANC-1 and SW1990, mouse pancreatic cancer cell line Pan02-mCherry, and mouse macrophage cell line RAW264.7 were purchased from the Cell Resource Center, Institute of Basic Medical Sciences, Chinese Academy of Medical Sciences and Peking Union Medical College. Cells were maintained at 37°C with 5% CO_2 in high-glucose Dulbecco's Modified Eagle Medium (DMEM, Invitrogen, USA), supplemented with 10% fetal bovine serum (FBS, Gibco, USA), 100 U/mL penicillin (Hyclone, USA), and 100 μg/mL streptomycin (Hyclone, USA). HHT was purchased from Xi'an Hao-Xuan Bio-Tech Co., Ltd. (Shanxi, China). The HHT powder was dissolved in dimethyl sulfoxide to prepare a 20 mM stock solution, which was further diluted to corresponding concentrations with DMEM complete medium for cellular experiments.

Healthy female C57BL/6 mice (6 – 8 weeks old) were purchased and bred at the animal center of the Institute of Basic Medical Sciences. All animal experiments reported were carried out in accordance with the guidelines of the committee on the Animal Care and Use of Institute of Basic Medical Sciences, Chinese Academy of Medical Sciences and Peking Union Medical College (Ethics Approval ID: ACUC-A02-2023-015). Mice were euthanized through cervical dislocation following isoflurane anesthesia in accordance with the 2020 AVMA Guidelines for the Euthanasia of Animals, ensuring humane treatment. The study adhered strictly to the ARRIVE guideline.[20]

2.2. Cell viability assay

PANC-1, SW1990, Pan02-mCherry, and RAW264.7 cells were seeded at a density of 5×10^3 cells per well and allowed to attach overnight. Subsequently, HHT concentrations ranging from 0 to 400 nM were added to the cells. After 24 or 48 h of treatment, 10 μL of cell counting kit-8 (CCK-8) reagent (Dojindo, Japan) was added, and the cells were incubated for an additional 1 – 4 h at 37°C. Absorbance was measured at 450 nm and 630 nm using a microplate reader (Thermofisher Scientific, USA). Cell viability was calculated as a percentage of the control, and the half-maximal inhibitory concentration (IC50) values were determined using GraphPad Prism software (GraphPad Software, USA).

2.3. Cell proliferation assay

PANC-1 cells were washed with phosphate-buffered saline (PBS) and resuspended in serum-free DMEM. Next, carboxyfluorescein succinimidyl ester (CFSE, Dojindo, Japan) was added to the cell suspension at 5 μM, followed

by incubation at 37°C for 10 min. Unbound CFSE was removed by centrifugation. The CFSE-labeled cells were then treated with various concentrations of HHT for 24 or 48 h. Fluorescence intensity was analyzed using an Accuri™ C6 flow cytometer (BD Biosciences, USA).

2.4. Colony-forming assay

PANC-1 and Pan02-mCherry cells were seeded into 6-well plates at a density of 2×10^3 cells per well. After overnight adherence, the cells were treated with HHT at different concentrations for 48 h, and then the culture medium was replaced with fresh medium and replenished every 3 days. After a 14-day incubation, cell colonies were fixed with 4% paraformaldehyde (PFA) and stained with crystal violet solution. The number of colonies was counted manually.

2.5. *In vivo* tumor-forming assay

Pan02-mCherry cells were cultured with HHT at 25 nM and 200 nM, respectively. After 24 h, the cells were collected, centrifuged, and counted. Untreated or HHT-treated cells were then subcutaneously injected into mice at a dose of 2×10^6/mouse, with four mice per group. Tumor sizes were recorded during the experiment. On the 23rd day post-implantation, *in vivo* imaging of mouse tumors was performed using the Xenogen IVIS Spectrum system (Caliper Life Sciences, USA). The mice were then sacrificed, and the tumors were excised and weighed.

2.6. Cell cycle assay

PANC-1 cells were treated with HHT at 25 nM, 50 nM, and 100 nM for 48 h, then collected, washed, and fixed with 70% ethanol overnight at −20°C. The cells were treated with RNase for 30 min at 37°C and stained with propidium iodide (PI) staining solution (BD Biosciences, USA) for 30 min. Flow cytometric analysis was performed using an Accuri™ C6 flow cytometer (BD Biosciences, USA), and the data were processed using ModFit LT™ software (Verity Software, USA).

2.7. Western blotting

PANC-1 cells were incubated with HHT at 50 nM and 100 nM for 48 h, then washed with cold PBS and lysed using RIPA buffer (Solarbio, China) supplemented with phenylmethylsulfonyl fluoride (PMSF, Solarbio, China) and protease inhibitors (Applygen, China). The cell lysates were centrifuged at 12,000 rpm for 15 min at 4°C, and the protein concentrations of the supernatants were determined using a BCA kit (Thermofisher Scientific, USA). Equal amounts of protein were separated on 12% SDS-PAGE gels and transferred onto 0.45 μm PVDF membranes (Merck Millipore, Germany). The membranes were blocked with 5% non-fat milk in Tris-buffered saline with 0.1% Tween-20 (TBST) for 1 h at room temperature, followed by incubation with primary antibodies overnight at 4°C. The primary antibodies used in this study included cyclin D2, cyclin-dependent kinase 1 (CDC2), cell division cycle 25c (CDC25c), p53, and GAPDH (Cell Signaling Technology, USA). After washing with TBST, the membranes were incubated with horseradish peroxidase-conjugated secondary antibodies (Biolegend, USA) for 1 h at room temperature. Protein bands were visualized using an enhanced chemiluminescence reagent (ECL, Merck Millipore, Germany) in a gel imaging system (Tanon, China). The blot quantification was performed using ImageJ software (NIH, USA). Protein expression levels were normalized to GAPDH, and relative protein expression levels were calculated.

2.8. Cytoskeleton staining assay

PANC-1 cells were treated with 50 nM HHT for 48 h. After fixation with 4% PFA, the cells were stained with Flash Phalloidin™ Red 594 (Biolegend, USA) for cytoskeleton visualization and DAPI (ZSGB-Bio, China) for nuclear staining. Cytoskeletons were observed using an Olympus FV1000MPE multiphoton laser scanning microscope (Olympus, Japan).

2.9. Intracellular ROS measurement

After treatment with HHT (50 nM, 100 nM) for various durations, PANC-1 cells were incubated with 10 μM 2',7'-dichlorodihydrofluorescein diacetate (DCFH-DA, Sigma, USA) for 30 min at 37°C. The fluorescence intensity, which represents the intracellular ROS level, was measured using a flow cytometer. Relative ROS levels were calculated by normalization to the control.

2.10. Cell OCR measurement

The OCR of PANC-1 cells was measured using an XFe24 extracellular flux analyzer (Agilent, USA). HHT-pretreated (50 nM, 24 h) and untreated cells were seeded into XFe24 cell culture microplates and allowed to adhere overnight. The medium was then replaced with XF base medium supplemented with glucose, pyruvate, and glutamine. OCR measurements were recorded after the sequential addition of oligomycin (oligo), carbonyl cyanide 4-(trifluoromethoxy) phenylhydrazone, and a combination of rotenone and antimycin A. The data were analyzed using Seahorse XFe24 software to determine basal respiration, adenosine triphosphate (ATP)-linked respiration, maximal respiration, and non-mitochondrial respiration.

2.11. ATP measurement

PANC-1 cells were treated with HHT at 50 nM and 100 nM for 24 or 48 h. ATP levels were measured using an ATP assay

kit (Beyotime, China) according to the manufacturer's instructions. Luminescence intensity was measured using a microplate reader (Thermofisher Scientific, USA) and normalized to the protein content of the cell lysates.

2.12. NAD^+/NADH measurement

PANC-1 cells were treated with HHT at 50 nM and 100 nM for 24 or 48 h. Intracellular total NAD (NAD_{total}) and NADH content were measured using a commercial assay kit (Beyotime, China) according to the manufacturer's protocol. The NAD^+/NADH ratio was calculated according to the following formula.

$$[NAD^+]/[NADH] = ([NAD_{total}] - [NADH])/[NADH]$$

2.13. *In vivo* therapeutic efficacy evaluation

First, an HHT toxicity assessment was conducted in healthy mice to determine a safe dosage for therapeutic evaluation. Briefly, healthy female C57BL/6 mice (6 – 8 weeks old, ~20 g) were randomly divided into five groups (n = 3). HHT solution was prepared in 0.4% (w/v) Soluplus® (BASF SE, Germany) in PBS, with four dosages including 0.5, 1, 2, and 4 mg/kg. A PBS solution containing 0.4% Soluplus® was used as the control. Mice were intravenously administered different dosages of HHT daily for four consecutive days. The survived mice were monitored and recorded daily for 5 days after the initial administration.

Pan02-mCherry cells were subcutaneously injected into the right axillary region of mice at the dose of 2×10^6 cells per mouse. When tumors reached about 75 mm^3, mice were randomly divided into three groups (n = 7). Meanwhile, HHT solution was prepared in 0.4% of Soluplus® (BASF SE, Germany) in PBS for the animal experiment. Mice were intravenously administered with HHT at the dosages of 0.5 and 1.0 mg/kg/day for 5 days/week over 2 weeks. The control (Ctrl) group received an injection of 0.4% of Soluplus® in PBS in the same volume. The body weight and tumor volume were measured. On the 3rd day after the final injection, mice were sacrificed, and tumors were excised, photographed, and weighed. Tumor samples were fixed in 4% PFA, embedded in paraffin, and analyzed with hematoxylin-eosin (H&E) staining and immunofluorescence staining for Ki67 and F4/80 (Servicebio, China) according to the manufacturer's instructions.

2.14. Statistical analysis

Statistical analyses were carried out using the GraphPad Prism software (version 10.1.1, GraphPad Software, USA). All data in this study were presented as mean ± standard deviation (SD). Comparisons between two groups were performed using an unpaired two-tailed Student's t-test. One-way analysis of variance (ANOVA) was used for comparisons among three or more groups defined by a single factor, whereas two-way ANOVA was used for comparisons involving two factors. The least significant difference *post hoc* test was conducted following ANOVA to compare group means. A $P < 0.05$ was considered statistically significant.

3. Results

3.1. HHT inhibited the growth and proliferation of PDAC cells *in vitro*

The cytotoxic effect of HHT on the viability of PDAC cells was evaluated using the CCK-8 assay. It was shown that the viability of PANC-1 cells was significantly inhibited by HHT in a dose- and time-dependent manner (Figure 1A). The IC50 value of HHT for PANC-1 at 24 hs was 23.11 nM. Similarly, the IC50 values for SW1990 cells and Pan02-mCherry cells at 24 h were 144.00 nM and 20.67 nM, respectively (Table S1). The effect of HHT on the proliferation of PANC-1 cells was examined using the CFSE

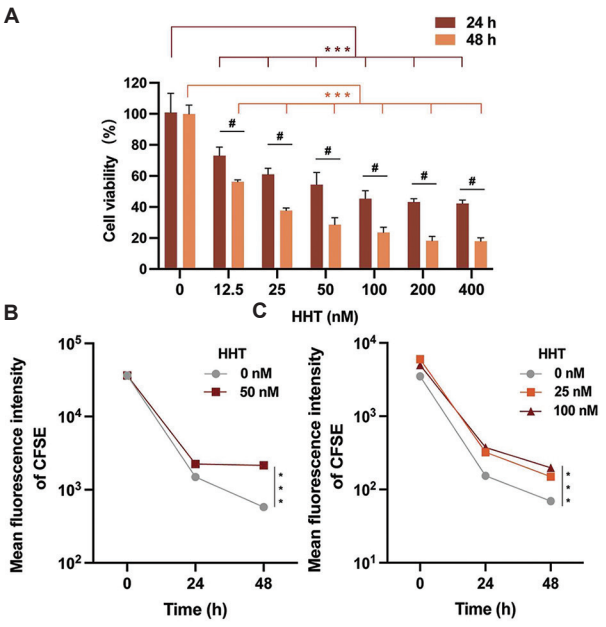


Figure 1. Effects of HHT on the viability and proliferation of pancreatic cancer cells. (A) Viability of human pancreatic cancer PANC-1 cells treated with HHT at different concentrations for 24 and 48 h, assessed by the CCK-8 assay (n = 4). (B) Proliferation of PANC-1 cells treated with HHT for 24 and 48 h, evaluated by CFSE staining assay (n = 3). PANC-1 cells were labeled with 5 μM CFSE, followed by HHT treatment at 50 nM for 24 and 48 h. (C) Long-term inhibitory effect of HHT on PANC-1 cell proliferation. Cells were pre-treated with 25 nM or 100 nM HHT for 24 h, followed by incubation in fresh, drug-free medium for another 24 and 48 h (n = 3). Note: #$P < 0.05$, ***$P < 0.001$.
Abbreviations: HHT: Homoharringtonine; CFSE: Carboxyfluorescein succinimidyl ester; CCK-8 assay: Cell counting kit-8 assay; h: Hours.

assay. The results showed that the fluorescent intensity of PANC-1 cells treated with HHT decreased much more slowly over time than that of the control (Figure 1B). Specifically, the mean fluorescent intensity of PANC-1 cells treated with 50 nM HHT was nearly 4-fold compared to the control. To determine whether the inhibitory effect persisted over time, PANC-1 cells were treated with HHT at 25 nM or 100 nM for 24 h, followed by replenishing with fresh complete medium and further incubated for another 24 or 48 h. Results showed that HHT-treated cells continued to exhibit significantly higher CFSE values, indicating that the inhibitory effect on proliferation was still evident 48 h after HHT removal (Figure 1C).

Next, crystal violet staining was used to investigate the effect of HHT on the colony-forming ability of PANC-1 and Pan02-mCherry cells. Both cell lines exhibited a significant reduction in colony formation after 48 h of incubation of HHT in a dose-dependent manner compared to untreated cells (Figure 2A). Specifically, in PANC-1 cells, 25 nM HHT inhibited colony formation by about 41%. Pan02-mCherry cells exhibited greater sensitivity to HHT treatment, with the same concentration inducing about 54% inhibition of colony formation in reference to that of control (Figure 2B). The inhibitory effect of HHT on the tumorigenic capacity of Pan02-mCherry cells was also examined *in vivo*. The tumor cells were treated with HHT at 200 nM for 24 h before implantation. On the 23rd post-implantation, the fluorescence intensity of the tumor mass in the HHT-pretreated group was lower than that of control group (Figure 2C), indicating that HHT-pretreated cells developed tumors more slowly than the control cells (Figure 2D). At the same time, the tumor weight in the HHT-pretreated group was significantly decreased compared to the control group.

3.2. HHT-induced oxidative stress and impaired mitochondrial respiration in PDAC cells

The intracellular ROS levels were measured using DCFH-DA in PANC-1 cells treated with HHT at 50 nM and 100 nM. Results showed that ROS levels remained unchanged during the first 6 h of HHT treatment but were significantly elevated after 12 h of treatment, demonstrating both dose- and time-dependent effects (Figure 3A). Notably, the ROS levels in the 100 nM group were much higher than those in the 50 nM group at 12, 24, and 48 h. Fluorescent microscopy of cells treated with HHT for 18 h (Figure 3B) confirmed these findings, showing increased cellular fluorescence with HHT treatment at both 50 nM and 100 nM, consistent with the data in Figure 3A. At the same time, NADH levels were downregulated following HHT treatment (Figure 3C), along with a significant increase of NAD^+/NADH ratio after 48 h of HHT treatment at 50 nM or 100 nM (Figure 3D), clearly indicating a state of oxidative stress.

To examine whether oxidative stress affected mitochondrial function in the tumor cells, OCR was

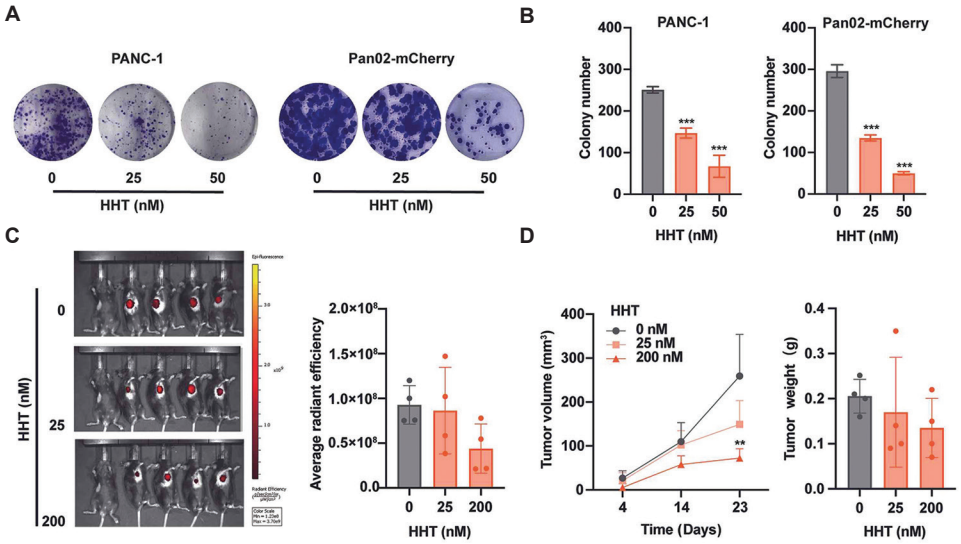


Figure 2. Effects of HHT on colony formation and tumorigenicity. (A) Representative images of cell colonies stained with crystal violet. PANC-1 and Pan02-mCherry cells were incubated in the complete medium for 14 days following treatment with 25 nM and 50 nM HTT for 48 h. (B) Quantification of colony formation in PANC-1 and Pan02-mCherry cells from the colony formation experiment in panel A ($n = 3$). ***$P < 0.001$. (C) Fluorescent imaging and intensity analysis of tumors *in vivo* on the 23rd day after inoculation. Cells were treated with 25 nM or 200 nM HTT for 24 h before inoculation. A healthy mouse without cancer cell injection was placed on the left of each image as a background control ($n = 4$). (D) Tumor volumes and weights in each group ($n = 4$).
Abbreviation: HHT: Homoharringtonine.

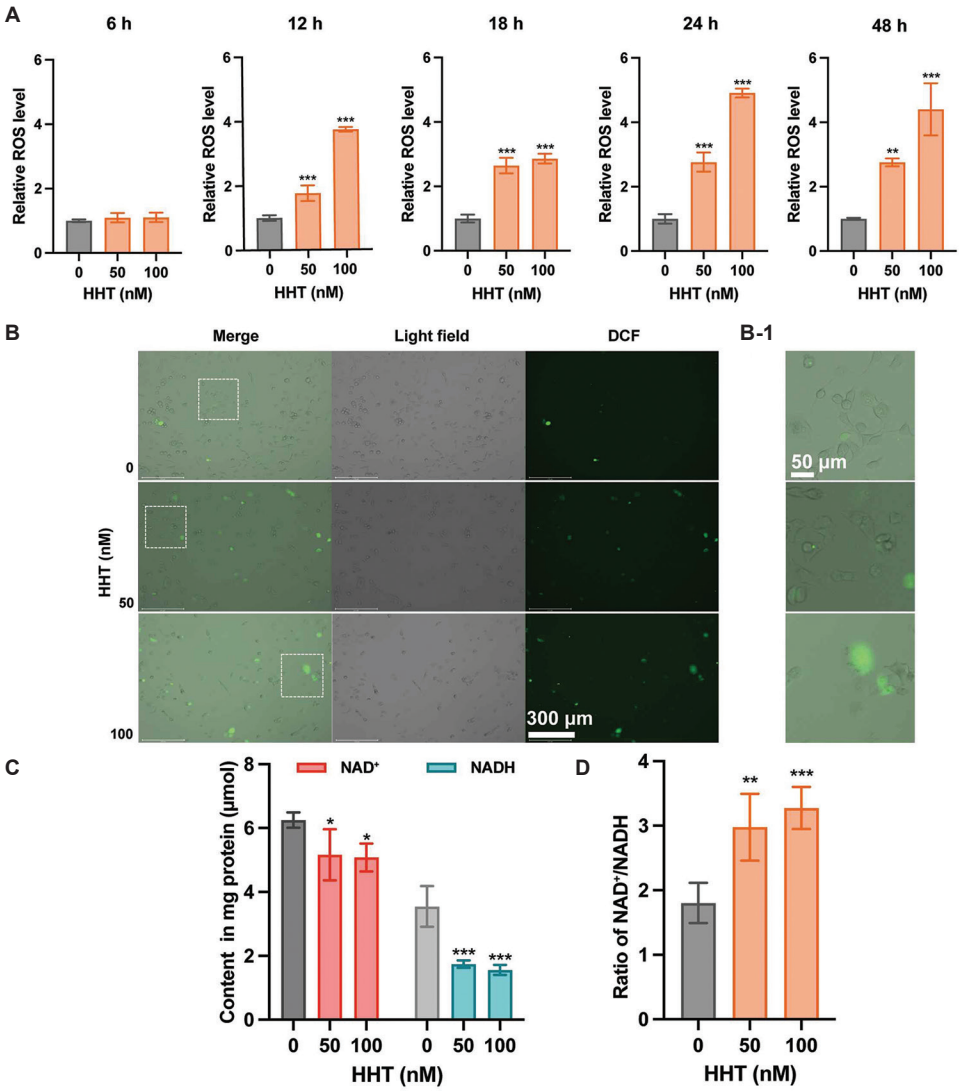


Figure 3. HHT-induced oxidative stress in PANC-1 cells. (A) Flow cytometric analysis of intracellular ROS in PANC-1 cells treated with 50 nM and 100 nM HHT at different time points (n = 3). (B) Fluorescence images of PANC-1 cells treated with 50 nM or 100 nM HHT for 18 h and stained with DCFH-DA. Panel B-1 presents a magnified view of the highlighted area in panel B, marked with dashed lines. Magnification: 4× and 12× for pane B and B1, respectively. (C) NAD^+ and NADH contents in PANC-1 cells treated with 50 nM and 100 nM HHT for 48 h (n = 4). (D) NAD^+/NADH ratio calculated from panel C. Note: $^*P < 0.05$, $^{**}P < 0.01$, $^{***}P < 0.001$.

Abbreviations: HHT: Homoharringtonine; ROS: Reactive oxygen species; NAD^+/NADH: Nicotinamide adenine dinucleotide; DCFH-DA: Dichlorodihydrofluorescein diacetate; DCF: 2′,7′-dichlorofluorescein; μmol: Micromole; h: Hours.

measured by the Seahorse XFe24 analyzer (Figure 4A). HHT treatment reduced the OCR to 61.15 pmol/min/10^4 cells, compared to 142.9 pmol/min/10^4 cells in the untreated group, indicating impaired mitochondrial respiration. Specifically, the OCR associated with ATP biosynthesis in HHT-treated cells dropped to 44.51 pmol/min/10^4 cells, compared to 109.4 pmol/min/10^4 cells in the control group, suggesting that HHT inhibited mitochondrial ATP production. Furthermore, the maximum respiration rate, as reflected by the OCR, of HHT-treated PANC-1 cells was notably lower, indicating a substantial decrease in energy generation capacity. Moreover, the spare respiratory capacity of these cells was extremely low (Figure 4B), reflecting the inability to adapt mitochondrial metabolism to stress conditions.[21] In addition, ATP levels in HHT-treated cells were measured using an ATP assay kit, showing significantly lower levels compared to those in control cells (Figure 4C), consistent with the OCR results. Taken together, HHT induced oxidative stress over time, which impaired mitochondrial respiration.

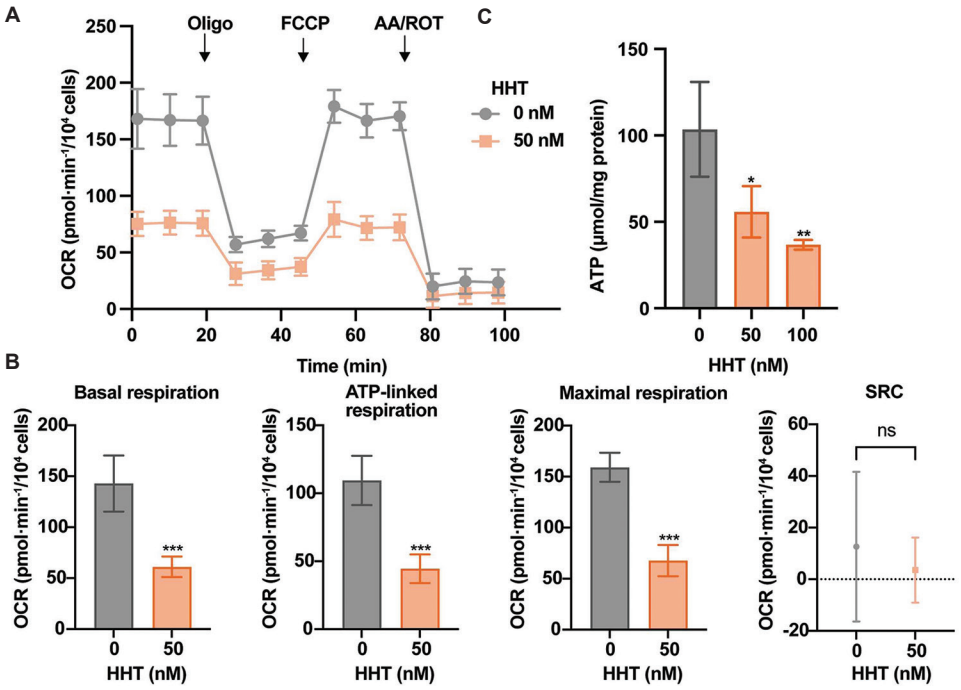


Figure 4. HHT inhibits mitochondrial respiration in PANC-1 cells. (A) OCR assay of HHT-treated cells using the Seahorse instrument (n = 5). (B) Basal OCR, ATP-linked respiration, maximal respiration, and spare respiratory capacity were calculated from OCR curves (n = 5). (C) ATP content in PANC-1 cells treated with 50 nM and 100 nM HHT for 48 h (n = 3). Note: $^{*}P < 0.05$, $^{**}P < 0.01$, $^{***}P < 0.001$.
Abbreviations: HHT: Homoharringtonine; OCR: Oxygen consumption rate; ATP: Adenosine triphosphate; Oligo: Oligomycin; FCCP: Carbonyl cyanide-p-(trifluoromethoxy) phenylhydrazone; AA/ROT: Antimycin A and rotenone; SRC: Spare respiratory capacity; pmol: Picomole; μmol: Micromole; min: Minutes; ns: Not significant.

3.3. HHT-induced cell cycle arrest

The effect of HHT on the cell cycle of PANC-1 cells treated with HHT for 48 h was investigated by flow cytometry. Results showed that HHT treatment induced cell cycle arrest in the S phase (Figure 5A). Concurrently, the expressions of CDC2, CDC25c, cyclinD2, and p53 in HHT-treated PANC-1 cells were downregulated in a dose-dependent manner (Figure 5B). Quantification results (Figure 5C), derived from the replicates of Western blotting (Figure S1-S8), revealed that nearly half of the CDC2, CDC25c, and Cyclin D2 protein levels were decreased by 50 nM of HHT. Notably, PANC-1 cells express mutant p53 (mp53 R273H), which has a reported positive correlation with CDC2 expression in PANC-1 cells.[22] Western blot analysis showed that HHT treatment significantly decreased the expression of mp53 in a dose-dependent manner, which is consistent with previously reported findings in the literature. Moreover, the effect of HHT on the cytoskeleton of PANC-1 cells was visualized using confocal microscopy. HHT-treated cells showed fewer actin fibers dispersed in the cells (Figure 5D), suggesting a connection between cytoskeletal alterations, inhibited cell division, and cell cycle arrest.

3.4. HHT-inhibited tumor growth and proliferation of PDAC cells *in vivo*

The therapeutic effect of HHT on pancreatic cancer was investigated using a mouse model subcutaneously inoculated with Pan02-mCherry cells. First, the toxicity of HHT was assessed in healthy mice (n = 3 per group) at four dosages, including 0.5 mg/kg, 1.0 mg/kg, 2.0 mg/kg, and 4.0 mg/kg (administered once per day for four consecutive days) to determine the appropriate dosages for therapeutic efficacy experiments. Doses of 0.5 mg/kg and 1.0 mg/kg did not induce mortality or obvious body weight loss during the experimental period. However, one mouse (1/3) in the 2 mg/kg group was found dead on the 4th day after the final injection, whereas all mice (3/3) in the 4 mg/kg group were found dead on the 1st day after the initial injection (Figure 6A and B). Based on these findings, 0.5 mg/kg and 1.0 mg/kg were selected for the therapeutics efficacy assay. The tumor-bearing mice were randomly divided into three groups (n = 7 per group) and intravenously administrated with HHT at 0.5 mg/kg, 1.0 mg/kg, or 0.4% of Soluplus® in PBS as the control. It was shown that HHT treatment significantly reduced the tumor volumes in a dose-dependent manner compared to the control group

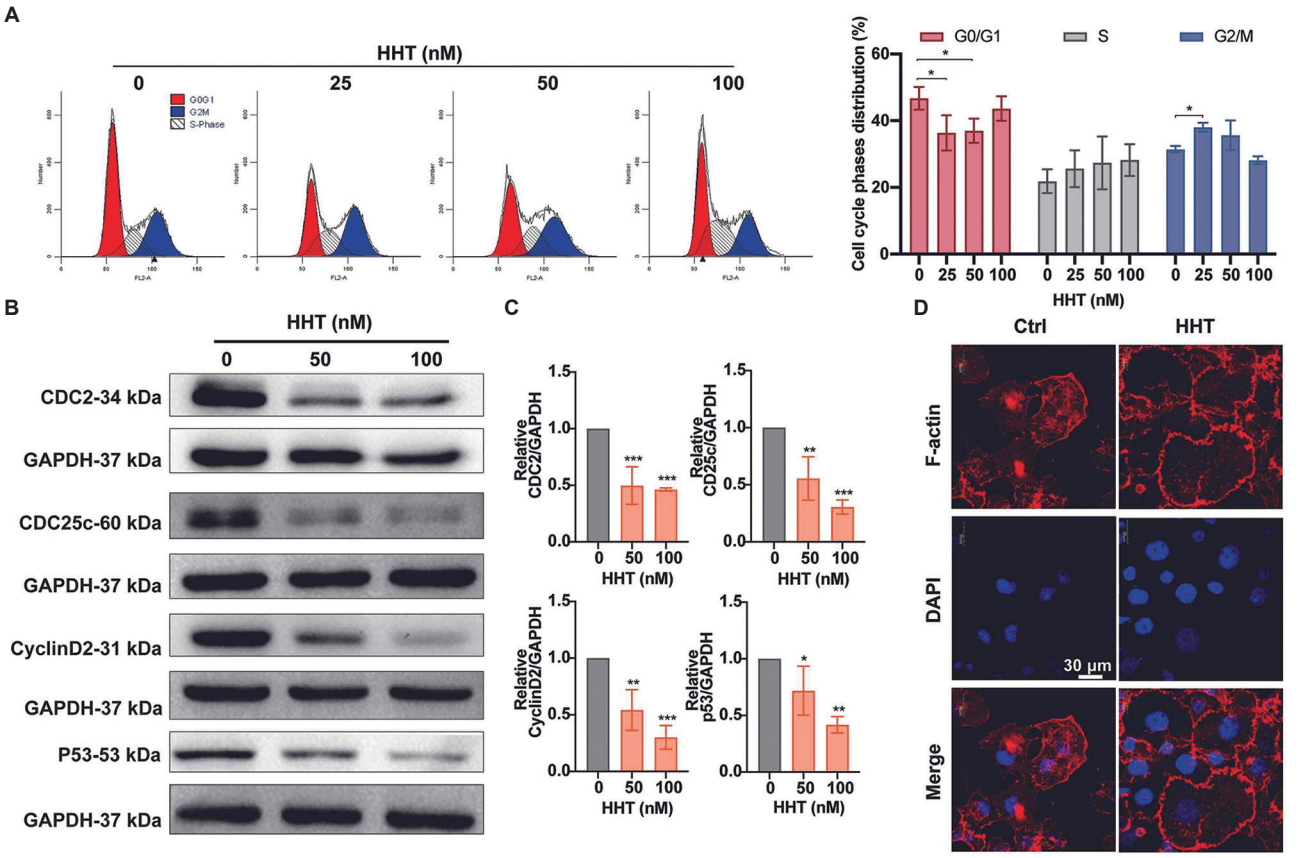
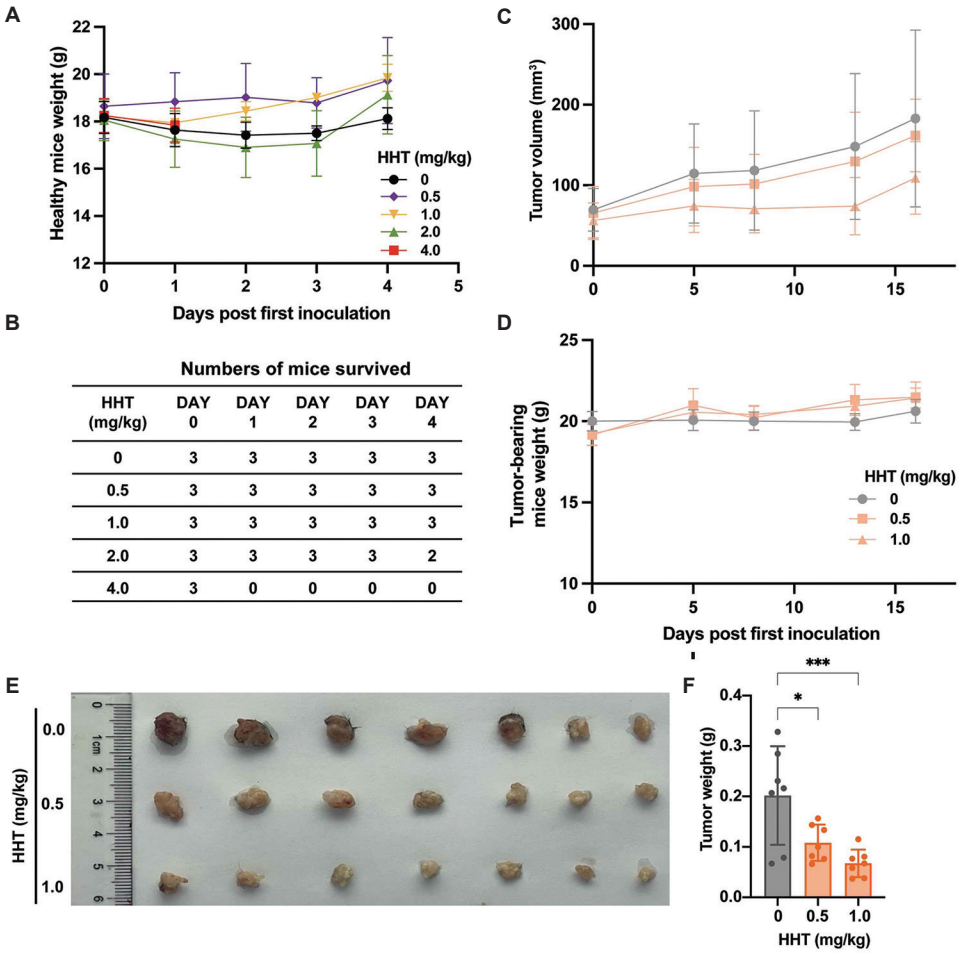


Figure 5. HHT-induced cell cycle arrest in PANC-1 cells. (A) Cell cycle analysis by flow cytometry and quantification of PANC-1 cells ($n = 3$). PANC-1 cells were treated with 25 nM, 50 nM, and 100 nM HHT for 48 h, followed by fixation and PI staining. (B) Expression levels and (C) quantification of CDC2, CDC25c, cyclin D2, and mutant p53 in PANC-1 cells treated with 50 nM and 100 nM HHT for 48 h ($n = 3$). Original blots for display and quantitation are presented in Figures S1 – S8 (supplementary file). (D) Cytoskeleton analysis of untreated (Ctrl) and or HHT-treated (50 nM, 48 h) PANC-1 cells. Actin was stained with phalloidin (red fluorescence), and nuclei were stained with DAPI (blue fluorescence). Magnification: 400× for panel D. Note: $^{*}P < 0.05$, $^{**}P < 0.01$, $^{***}P < 0.001$.

Abbreviations: HHT: Homoharringtonine; PI: Propidium iodide; CDC2: Cyclin-dependent kinase 1: CDC25c: Cell division cycle 25c; Ctrl: Control.

(Figure 6C). Concurrently, body weight measurements indicated that neither 0.5 mg/kg nor 1.0 mg/kg of HHT caused significant weight loss or systemic toxicity in mice (Figure 6D). On the 16th day after the initial HHT administration, all mice were euthanized, and the tumors from the three groups were excised, photographed, and weighed. Tumor sizes in the HHT-treated groups were notably smaller compared to those in the control group (Figure 6E). Quantification analysis of tumor weights further confirmed the inhibitory effect of HHT on tumor growth (Figure 6F).

H&E staining of tumor sections revealed that HHT treatment significantly inhibited the proliferation of pancreatic cancer cells. In the control mice, pancreatic cancer foci were observed, characterized by typical ductal carcinoma structures (asterisks) mainly distributed at the edges of the tissues. Following HHT treatment, the number of pancreatic cancer foci decreased significantly. In the mice treated with 0.5 mg/kg of HHT, tumor cells in the ductal structures were shrunken in size (asterisks) and surrounded by fibrous structures. For the 1.0 mg/kg HHT-treated group, only a few ductal carcinoma foci were observed. The tumor cells in these structures displayed unclear boundaries and lacked nuclei (asterisks), suggesting cell death (Figure 7A). Ki67 immunofluorescence staining of tumor sections further confirmed the reduced cell proliferation with HHT treatment. The Ki67-positive cells (red fluorescence) were clearly seen in the control group, whereas their numbers decreased progressively with increasing doses of HHT, demonstrating a dose-dependent reduction of tumor cell proliferation (Figure 7B). The above results show that HHT inhibits pancreatic tumor growth *in vivo* by suppressing cell proliferation.



HHT (mg/kg)	DAY 0	DAY 1	DAY 2	DAY 3	DAY 4
0	3	3	3	3	3
0.5	3	3	3	3	3
1.0	3	3	3	3	3
2.0	3	3	3	3	2
4.0	3	0	0	0	0

Figure 6. Toxicity evaluation and therapeutic effects of HHT on pancreatic cancer *in vivo*. (A) Body weight of healthy mice received intravenous administration of HHT at four dosages including 0.5 mg/kg, 1.0 mg/kg, 2.0 mg/kg, and 4.0 mg/kg (once per day for 4 days) (n = 3). (B) Numbers of surviving mice after receiving the treatment described in panel A. (C) Tumor volume growth curve for each group. The tumor-loading mice were given a 2-week treatment. Each week, HHT at 0.5 mg/kg and 1.0 mg/kg were administered once per day for five consecutive days, followed by a 2-day break. (D) Body weight change curve for the three groups. (E) Representative tumor images from each group after 2 weeks of HHT treatment. On the day 16, all tumors were collected and analyzed. (F) Tumor weights of mice in each group (n = 7). Note: $^{*}P < 0.05$, $^{***}P < 0.001$.
Abbreviations: HHT: Homoharringtonine; g: Gram.

3.5. HHT alleviated immunosuppressive status within the TME

To further assess whether HHT affected the TME, the viability of RAW264.7 macrophages was examined using the CCK-8 assay. It was shown that HHT treatment led to a dose-dependent reduction in macrophage viability (Figure 8A), with an IC50 of 52.33 nM. Immunofluorescence staining indicated that the number of macrophages was reduced by the HHT treatment. In the control group, a large amount of F4/80-positive macrophages (green fluorescence) were distributed and surrounded the ductal carcinoma structures. However, treatment with 1.0 mg/kg HHT significantly decreased the number of macrophages in the tumor tissues (Figure 8B).

4. Discussion

PDAC is a highly invasive and deadly malignant tumor.[23] Although current standard-of-care treatments such as FOLFIRINOX (a combination of 5-fluorouracil, leucovorin, irinotecan, and oxaliplatin) and gemcitabine with nanoparticle albumin-bound paclitaxel (nab-paclitaxel) have achieved great progress in PDAC therapy,[4] clinical outcomes remain unsatisfactory. Therefore, it is of great significance to develop more effective chemotherapeutic drugs and understand their underlying mechanisms.

Previous studies have reported the inhibitory effects of HHT on the proliferation of certain pancreatic cancer cell lines, focusing primarily on signaling pathway activation

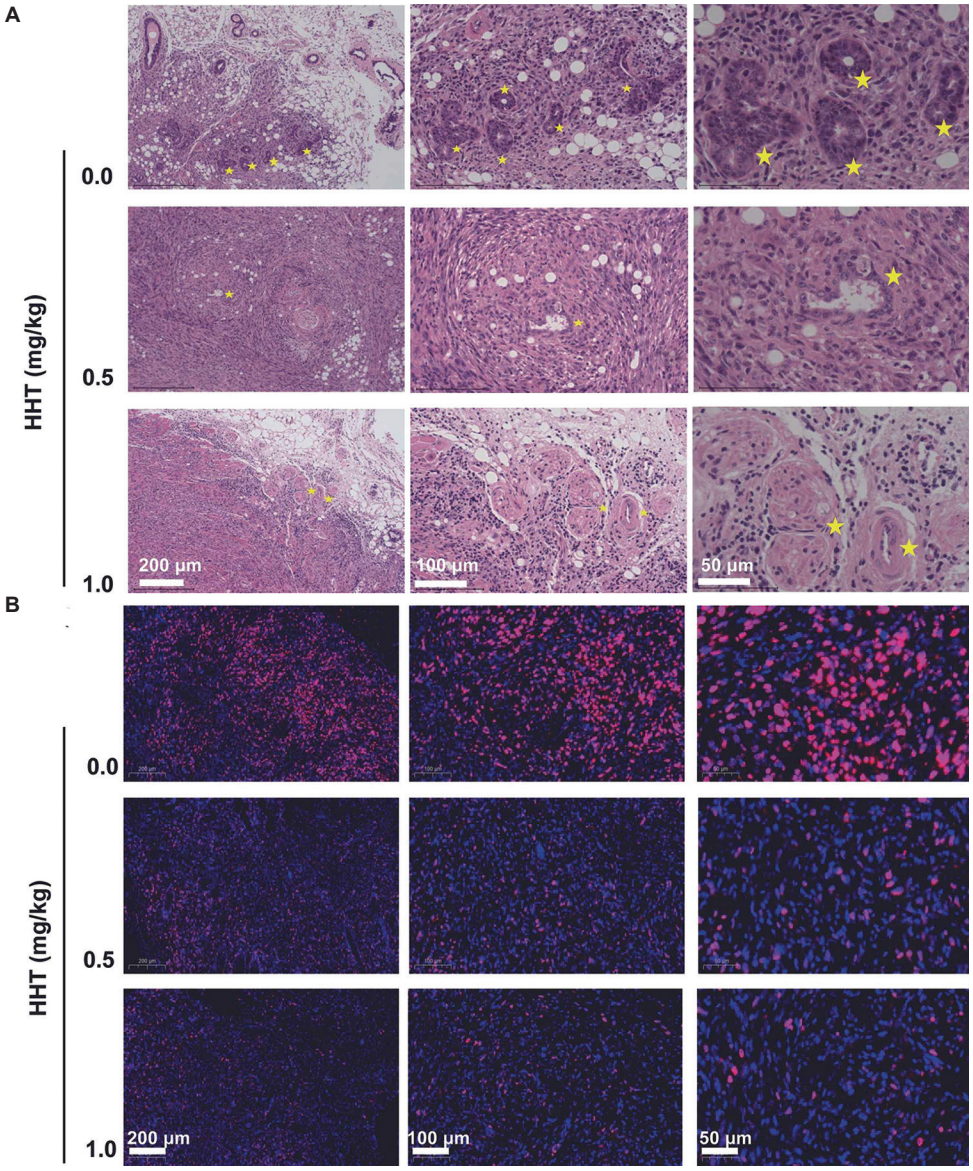


Figure 7. HHT inhibits the proliferation of pancreatic tumor cells *in vivo*. (A) Representative H&E-stained images of pancreatic tumor tissues treated with different dosages of HHT. Pancreatic cancer foci were indicated by yellow stars. Magnification: 10×, 20×, and 40×, respectively, from left to right for panel A. (B) Representative images of Ki67-stained cells in the pancreatic tumor tissues treated with different dosages of HHT. Ki67-positive cells showed red fluorescence, while nuclei were stained with DAPI in blue fluorescence. Magnification: 5×, 10×, and 20×, respectively, from left to right for panel B. Abbreviation: HHT: Homoharringtonine.

and cell cycle arrest. However, the mechanisms of HHT's action against pancreatic cancer have not been adequately investigated.

In this study, the therapeutic effect of HHT was investigated from the perspective of energy tumor cell energy metabolism to provide new insights into its underlying mechanisms. Chemotherapies have been widely recognized to increase intracellular ROS levels, disrupting cellular redox balance and damaging organelles.[24-27] Previous studies have shown that combining HHT with etoposide increased ROS-mediated cytotoxicity in AML cells,[28] whereas HHT inhibited mitochondrial complex I activity and OCR in CML cells.[16] Similarly, in 5-FU-resistant rectal cancer cells, HHT reduced OCR, mitochondrial complex I activity, and ATP production.[29] Experimental results further suggest that mitochondrial ROS could serve as a therapeutic target for pancreatic cancer cells. HHT-induced upregulation of ROS impaired mitochondrial respiration in PANC-1 cells. As mitochondria function as the "energy factories" within the cell, producing ATP essential to maintain normal physiological functions,[30]

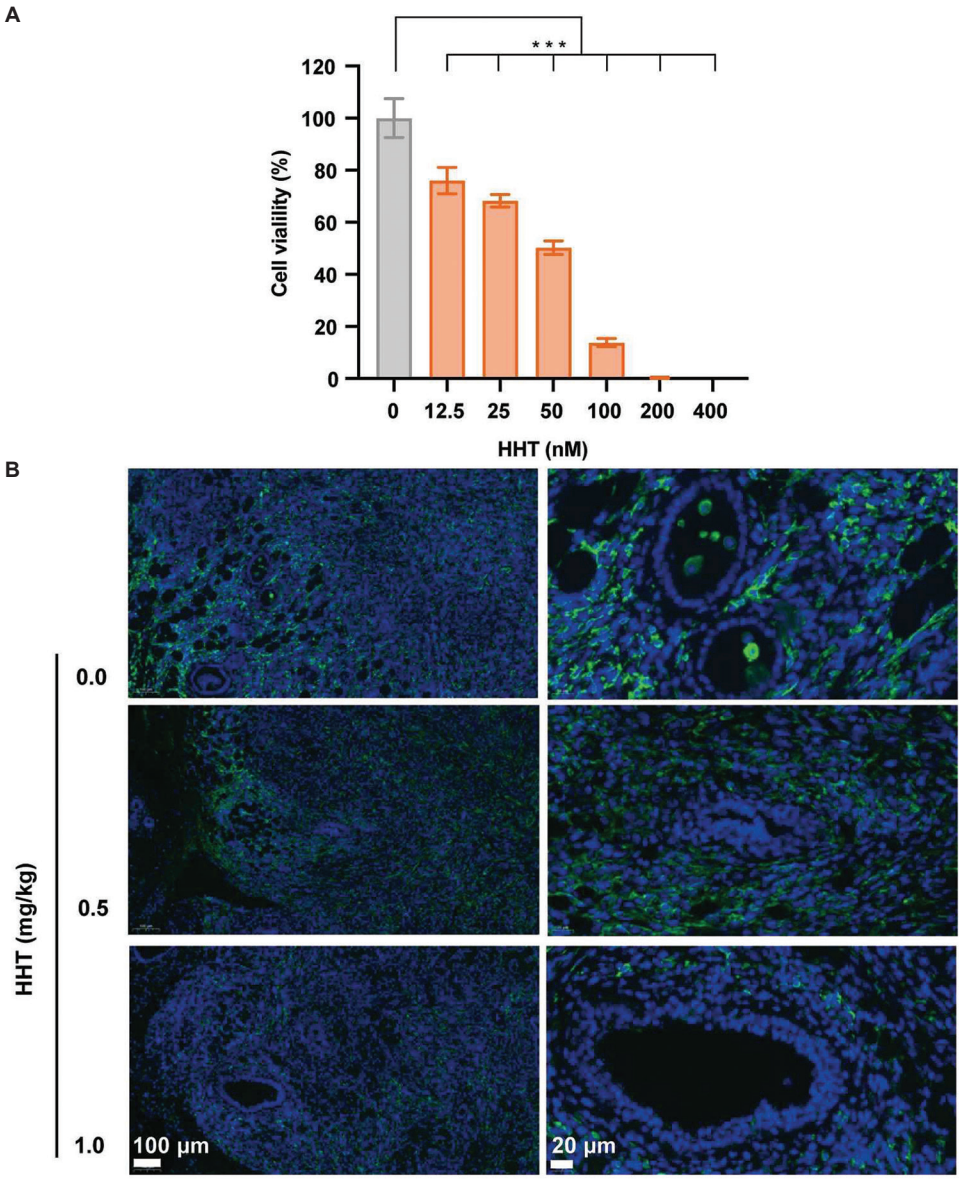


Figure 8. HHT alters the tumor microenvironment by inhibiting macrophages. (A) Viability of RAW264.7 cells incubated with HHT for 24 h, was measured by the CCK-8 assay (n = 4). (B) Representative images of tumor tissue stained with F4/80 (green fluorescence) and DAPI (blue fluorescence). Magnification: 10× and 40×, respectively, from left to right for panel B. Note: ***$P < 0.001$.
Abbreviations: HHT: Homoharringtonine; CCK-8 assay: Cell counting kit-8 assay.

the observed reduction in OCR following HHT treatment indicated inhibition of mitochondrial energy metabolism. This impairment rendered PANC-1 cells unable to adapt to mitochondrial dysfunction, thus inhibiting their proliferation. Taken together, targeting mitochondrial energy metabolism may serve as a promising therapeutic strategy for pancreatic cancer.

The present study also showed that the cell cycles of PANC-1 cells were arrested, accompanied by the dose-dependent downregulation of CDC2, CDC25c, and cyclin D2. In addition, HHT treatment reduced the expression of mutant p53 (mp53) in PANC-1 cells. Mutant p53 has been shown to have potential gain-of-function activities, such as interference with the regulation of cell survival, DNA damage repair, and drug resistance, in contrast to the tumor-suppressive roles of wild-type p53.[31,32] Previous studies have shown a positive correlation between mp53 and CDC2[33] in PANC-1 cells,[22] as well as in breast metastatic cancer cell line SKBR3, and head and neck cancer cell lines CAL27 and FADU.[34] It is known that

p53 and checkpoint protein kinases checkpoint kinase 1 (CHK1) and checkpoint kinase 2 (CHK2) regulate the phosphorylation of CDC25c, inhibiting its activity during DNA damage. This results in the breakdown of CDC25c in the cytoplasm, prevents the activation of the cyclin B1/CDK1 complex, and induces G2/M phase cell cycle arrest.[35-37] In this study, the downregulation of mp53 by HHT treatment may be associated with its impact on cell cycle proteins.

Moreover, pancreatic cancer is well-known for its characteristic immunosuppressive TME, which includes a large population of macrophages and fibroblasts. This study revealed that macrophages were more sensitive to HHT than PANC-1 cells, suggesting that HHT might alleviate the TME. Tumor-associated macrophages are widely recognized for their role in facilitating the TME,[38,39] which may contribute to the inhibitory effect of HHT on pancreatic cancer progression. In addition, this effect may promote the therapeutic efficacy of pancreatic cancer treatments when combined with other existing drugs. Although no clear mechanisms have been established, prior investigations have shown signs of HHT sensitizing other chemotherapeutic drugs in immunosuppressive cancers. For example, HHT acts synergistically with paclitaxel to combat triple-negative breast cancer cell lines[40] and sensitizes resistant human colorectal carcinoma cells to tumor necrosis factor-related apoptosis-inducing ligand-induced apoptosis.[41]

5. Conclusion

HHT showed potent antiproliferative effects on pancreatic cancer by inducing ROS elevation, impairing mitochondrial energy metabolism, and causing cell cycle arrest. In addition, it reduced macrophages in the TME to alleviate the immunosuppressive status. These findings suggest that HHT could potentially serve as a novel therapeutic agent for this devastating disease. Investigating the long-term effects of HHT on PDAC relapse and its efficacy in combination with other existing drugs is worthy of future studies.

Acknowledgments

The confocal microscopy was performed at the Core Labs, Institute of Basic Medical Sciences Chinese Academy of Medical Sciences. The optical small animal imaging was performed at the State Key Laboratory of Common Mechanism Research of Major Disease Platform. We would like to thank the lab personnel for their help in data collection.

Funding

This work was supported by CAMS Innovation Fund for Medical Science (CIFMS 2021-I2M-1-026), Haihe Laboratory of Cell Ecosystem Innovation Fund (22HHXBSS00040) and Beijing Natural Science Foundation (7244372).

Conflict of interest

The authors declare they have no competing interests.

Author contributions

Conceptualization: Haiyan Xu
Formal analysis: Xiaoxia Wang
Funding acquisition: Haiyan Xu
Methodology: Xiaoxia Wang, Tao Wang, Jie Meng, Xuelu Peng, Ke Zhu, Ming Ye
Project administration: Haiyan Xu
Resources: Haiyan Xu
Supervision: Haiyan Xu
Validation: Xiaoxia Wang, Tao Wang
Writing – original draft: Jie Meng, Xiaoxia Wang
Writing – review & editing: Haiyan Xu, Tao Wang

Ethics approval and consent to participate

All the animal experiments reported were carried out in accordance with the guidelines stipulated by the committee on the Animal Care and Use of Institute of Basic Medical Sciences, Chinese Academy of Medical Sciences and Peking Union Medical College (Ethics Approval ID: ACUC-A02-2023-015). Mice were euthanized using cervical dislocation following isoflurane anesthesia, in accordance with the 2020 AVMA Guidelines for the Euthanasia of Animals to ensure humane treatment.

Consent for publication

Not applicable.

Availability of data

The datasets used and analyzed during the current study are available from the corresponding author upon reasonable request.

References

1. Cai J, Chen H, Lu M, *et al*. Advances in the epidemiology of pancreatic cancer: Trends, risk factors, screening, and prognosis. *Cancer Lett*. 2021;520:1-11.

   doi: 10.1016/j.canlet.2021.06.027

2. Bray F, Laversanne M, Sung H, *et al*. Global cancer statistics 2022: GLOBOCAN estimates of incidence and mortality worldwide for 36 cancers in 185 countries. *CA Cancer J Clin*. 2024;74(3):229-263.

   doi: 10.3322/caac.21834

3. Connor AA, Gallinger S. Pancreatic cancer evolution and

heterogeneity: Integrating omics and clinical data. *Nat Rev Cancer*. 2022;22(3):131-142.

doi: 10.1038/s41568-021-00418-1

4. Christenson ES, Jaffee E, Azad NS. Current and emerging therapies for patients with advanced pancreatic ductal adenocarcinoma: A bright future. *Lancet Oncol*. 2020;21(3):e135-e145.

doi: 10.1016/S1470-2045(19)30795-8

5. Niu N, Shen X, Wang Z, *et al*. Tumor cell-intrinsic epigenetic dysregulation shapes cancer-associated fibroblasts heterogeneity to metabolically support pancreatic cancer. *Cancer Cell*. 2024;42(5):869-884.e9.

doi: 10.1016/j.ccell.2024.03.005

6. Raghavan S, Winter PS, Navia AW, *et al*. Microenvironment drives cell state, plasticity, and drug response in pancreatic cancer. *Cell*. 2021;184(25):6119-6137.e26.

doi: 10.1016/j.cell.2021.11.017

7. Li E, Cheung HCZ, Ma S. CTHRC1^{+} fibroblasts and SPP1^{+} macrophages synergistically contribute to pro-tumorigenic tumor microenvironment in pancreatic ductal adenocarcinoma. *Sci Rep*. 2024;14(1):17412.

doi: 10.1038/s41598-024-68109-z

8. Spratlin J, Sangha R, Glubrecht D, *et al*. The absence of human equilibrative nucleoside transporter 1 is associated with reduced survival in patients with gemcitabine-treated pancreas adenocarcinoma. *Clin Cancer Res*. 2004;10(20):6956-6961.

doi: 10.1158/1078-0432.CCR-04-0224

9. Fresno M, Jiménez A, Vázquez D. Inhibition of translation in eukaryotic systems by harringtonine. *Eur J Biochem*. 1977;72(2):323-330.

doi: 10.1111/j.1432-1033.1977.tb11256.x

10. Baaske DM, Heinstein P. Cytotoxicity and cell cycle specificity of homoharringtonine. *Antimicrob Agents Chemother*. 1977;12(2):298-300.

doi: 10.1128/AAC.12.2.298

11. Kantarjian HM, O'Brien S, Cortes J. Homoharringtonine/omacetaxine mepesuccinate: The long and winding road to food and drug administration approval. *Clin Lymphoma Myeloma Leuk*. 2013;13(5):530-533.

doi: 10.1016/j.clml.2013.03.017

12. Powell RG, Weisleder D, Smith CR, Rohwedder WK. Structures of harringtonine, isoharringtonine, and homoharringtonine. *Tetrahedron Lett*. 1970;(11):815-818.

doi: 10.1016/s0040-4039(01)97839-6

13. Wang L, Zhao L, Wei G, *et al*. Homoharringtonine could induce quick protein synthesis of PSMD11 through activating MEK1/ERK1/2 signaling pathway in pancreatic cancer cells. *J Cell Biochem*. 2018;119(8):6644-6656.

doi: 10.1002/jcb.26847

14. Fountzilas G, Lim LO, Yunis AA. The inhibitory effects of teniposide and homoharringtonine on the growth of pancreatic carcinoma cells *in vitro*. *Anticancer Res*. 1988;8(3):343-346.

15. Sarwar A, Zhu Z, Zhu M, *et al*. Homoharringtonine sensitizes pancreatic cancer to erlotinib by direct targeting and miRNA-130b-3p-mediated EphB4-JAK2-STAT3 axis. *J Pharm Pharmacol*. 2023;75(10):1294-1309.

doi: 10.1093/jpp/rgad055

16. Han H, Zhao C, Liu M, *et al*. Mitochondrial complex I inhibition by homoharringtonine: A novel strategy for suppression of chronic myeloid leukemia. *Biochem Pharmacol*. 2023;218:115875.

doi: 10.1016/j.bcp.2023.115875

17. Jeong KY, Sim JJ, Park M, Kim HM. Accumulation of poly (adenosine diphosphate-ribose) by sustained supply of calcium inducing mitochondrial stress in pancreatic cancer cells. *World J Gastroenterol*. 2022;28(27):3422-3434.

doi: 10.3748/wjg.v28.i27.3422

18. Zhu X, Zhang Y, Wang Y, *et al*. Agrimoniin sensitizes pancreatic cancer to apoptosis through ROS-mediated energy metabolism dysfunction. *Phytomedicine*. 2022;96:153807.

doi: 10.1016/j.phymed.2021.153807

19. Xia S, Miao Y, Liu S. Withaferin A induces apoptosis by ROS-dependent mitochondrial dysfunction in human colorectal cancer cells. *Biochem Biophys Res Commun*. 2018;503(4):2363-2369.

doi: 10.1016/j.bbrc.2018.06.162

20. Percie du Sert N, Ahluwalia A, Alam S, *et al*. Reporting animal research: Explanation and elaboration for the ARRIVE guidelines 2.0. *PLoS Biol*. 2020;18(7):e3000411.

doi: 10.1371/journal.pbio.3000411

21. Marchetti P, Fovez Q, Germain N, Khamari R, Kluza J. Mitochondrial spare respiratory capacity: Mechanisms, regulation, and significance in non-transformed and cancer cells. *FASEB J*. 2020;34(10):13106-13124.

doi: 10.1096/fj.202000767R

22. Fiorini C, Cordani M, Padroni C, Blandino G, Di Agostino S, Donadelli M. Mutant p53 stimulates chemoresistance of pancreatic adenocarcinoma cells to gemcitabine. *Biochim Biophys Acta*. 2015;1853(1):89-100.

doi: 10.1016/j.bbamcr.2014.10.003

23. Rahib L, Smith BD, Aizenberg R, Rosenzweig AB, Fleshman JM, Matrisian LM. Projecting cancer incidence and deaths to 2030: The unexpected burden of thyroid,

liver, and pancreas cancers in the United States. *Cancer Res*. 2014;74(11):2913-2921.

doi: 10.1158/0008-5472.CAN-14-0155

24. Liu J, He X, Deng S, *et al*. QDPR deficiency drives immune suppression in pancreatic cancer. *Cell Metab*. 2024;36(5):984-999.e8.

doi: 10.1016/j.cmet.2024.03.015

25. Tintelnot J, Xu Y, Lesker TR, *et al*. Microbiota-derived 3-IAA influences chemotherapy efficacy in pancreatic cancer. *Nature*. 2023;615(7950):168-174.

doi: 10.1038/s41586-023-05728-y

26. Zhang W, Gong M, Zhang W, *et al*. Thiostrepton induces ferroptosis in pancreatic cancer cells through STAT3/GPX4 signalling. *Cell Death Dis*. 2022;13(7):630.

doi: 10.1038/s41419-022-05082-3

27. Badgley MA, Kremer DM, Maurer HC, *et al*. Cysteine depletion induces pancreatic tumor ferroptosis in mice. *Science*. 2020;368(6486):85-89.

doi: 10.1126/science.aaw9872

28. Zhang J, Geng H, Liu L, Zhang H. Synergistic cytotoxicity of homoharringtonine and etoposide in acute myeloid leukemia cells involves disrupted antioxidant defense. *Cancer Manag Res*. 2019;11:1023-1032.

doi: 10.2147/CMAR.S187597

29. Chenghao H, Xuefeng L, Junli P, *et al*. Mitochondrial-targeting strategies with homoharringtonine: A novel approach for chemoresistant rectal cancer. *Biochem Biophys Res Commun*. 2025;743:151141.

doi: 10.1016/j.bbrc.2024.151141

30. Nunnari J, Suomalainen A. Mitochondria: In sickness and in health. *Cell*. 2012;148(6):1145-1159.

doi: 10.1016/j.cell.2012.02.035

31. Bullock AN, Fersht AR. Rescuing the function of mutant p53. *Nat Rev Cancer*. 2001;1(1):68-76.

doi: 10.1038/35094077

32. Acin S, Li Z, Mejia O, Roop DR, El-Naggar AK, Caulin C. Gain-of-function mutant p53 but not p53 deletion promotes head and neck cancer progression in response to oncogenic K-ras. *J Pathol*. 2011;225(4):479-489.

doi: 10.1002/path.2971

33. Di Agostino S, Strano S, Emiliozzi V, *et al*. Gain of function of mutant p53: The mutant p53/NF-Y protein complex reveals an aberrant transcriptional mechanism of cell cycle regulation. *Cancer Cell*. 2006;10(3):191-202.

doi: 10.1016/j.ccr.2006.08.013

34. Di Agostino S, Sorrentino G, Ingallina E, *et al*. YAP enhances the pro-proliferative transcriptional activity of mutant p53 proteins. *EMBO Rep*. 2016;17(2):188-201.

doi: 10.15252/embr.201540488

35. Winters ZE, Ongkeko WM, Harris AL, Norbury CJ. p53 regulates Cdc2 independently of inhibitory phosphorylation to reinforce radiation-induced G2 arrest in human cells. *Oncogene*. 1998;17(6):673-684.

doi: 10.1038/sj.onc.1201991

36. Le Gac G, Estève PO, Ferec C, Pradhan S. DNA damage-induced down-regulation of human Cdc25C and Cdc2 is mediated by cooperation between p53 and maintenance DNA (cytosine-5) methyltransferase 1. *J Biol Chem*. 2006;281(34):24161-24170.

doi: 10.1074/jbc.M603724200

37. Thanasoula M, Escandell JM, Suwaki N, Tarsounas M. ATM/ATR checkpoint activation downregulates CDC25C to prevent mitotic entry with uncapped telomeres. *EMBO J*. 2012;31(16):3398-3410.

doi: 10.1038/emboj.2012.191

38. Lin Y, Xu J, Lan H. Tumor-associated macrophages in tumor metastasis: Biological roles and clinical therapeutic applications. *J Hematol Oncol*. 2019;12(1):76.

doi: 10.1186/s13045-019-0760-3

39. Wang Y, Johnson KCC, Gatti-Mays ME, Li Z. Emerging strategies in targeting tumor-resident myeloid cells for cancer immunotherapy. *J Hematol Oncol*. 2022;15(1):118.

doi: 10.1186/s13045-022-01335-y

40. Plett R, Mellor P, Kendall S, *et al*. Homoharringtonine demonstrates a cytotoxic effect against triple-negative breast cancer cell lines and acts synergistically with paclitaxel. *Sci Rep*. 2022;12(1):15663.

doi: 10.1038/s41598-022-19621-7

41. Beranova L, Pombinho AR, Spegarova J, *et al*. The plant alkaloid and anti-leukemia drug homoharringtonine sensitizes resistant human colorectal carcinoma cells to TRAIL-induced apoptosis via multiple mechanisms. *Apoptosis*. 2013;18(6):739-750.

doi: 10.1007/s10495-013-0823-9